

# A Measurement Framework for Explicit and Implicit Urban Traffic Sensing

ZHOU QIN and ZHIHAN FANG, Rutgers University, USA

YUNHUAI LIU, Peking University, China

CHANG TAN, iFlytek, China

DESHENG ZHANG, Rutgers University, USA

Urban traffic sensing has been investigated extensively by different real-time sensing approaches due to important applications such as navigation and emergency services. Basically, the existing traffic sensing approaches can be classified into two categories by sensing natures, i.e., explicit and implicit sensing. In this article, we design a measurement framework called EXIMIUS for a large-scale data-driven study to investigate the strengths and weaknesses of two sensing approaches by using two particular systems for traffic sensing as concrete examples. In our investigation, we utilize TB-level data from two systems: (i) GPS data from five thousand vehicles, (ii) signaling data from three million cellphone users, from the Chinese city Hefei. Our study adopts a widely used concept called crowdedness level to rigorously explore the impacts of contexts on traffic conditions including population density, region functions, road categories, rush hours, holidays, weather, and so on, based on various context data. We quantify the strengths and weaknesses of these two sensing approaches in different scenarios and then we explore the possibility of unifying two sensing approaches for better performance by using a truth discovery-based data fusion scheme. Our results provide a few valuable insights for urban sensing based on explicit and implicit data from transportation and telecommunication domains.

CCS Concepts: • Networks → Network measurement; Sensor networks;

Additional Key Words and Phrases: Cellular networks, vehicular networks, measurement, truth discovery

**ACM Reference format:**

Zhou Qin, Zhihan Fang, Yunhuai Liu, Chang Tan, and Desheng Zhang. 2021. A Measurement Framework for Explicit and Implicit Urban Traffic Sensing. *ACM Trans. Sen. Netw.* 17, 4, Article 47 (August 2021), 27 pages.

<https://doi.org/10.1145/3461840>

47

---

This work is partially supported by NSF 1849238 and 1932223, National Key R&D Program of China 2018YFB2100300 and 2018YFB0803400, and National Natural Science Foundation of China (NSFC) 61925202 and 61772046.

Authors' addresses: Z. Qin, Rutgers University, 96 Frelinghuysen Rd, Piscataway, NJ, 08854, USA; email: zq58@cs.rutgers.edu; Z. Fang and D. Zhang, Rutgers University, 96 Frelinghuysen Rd, Piscataway, USA; emails: {zhihan.fang, desheng.zhang}@cs.rutgers.edu; Y. Liu, Peking University, 5 Yiheyuan Rd, Beijing, Beijing Shi, China; email: yunhuai.liu@pku.edu.cn; C. Tan, iFlytek, No. 666, Wangjiang Road West, Hefei, Anhui, China; email: changtan2@iflytek.com.

Permission to make digital or hard copies of all or part of this work for personal or classroom use is granted without fee provided that copies are not made or distributed for profit or commercial advantage and that copies bear this notice and the full citation on the first page. Copyrights for components of this work owned by others than the author(s) must be honored. Abstracting with credit is permitted. To copy otherwise, or republish, to post on servers or to redistribute to lists, requires prior specific permission and/or a fee. Request permissions from [permissions@acm.org](mailto:permissions@acm.org).

© 2021 Copyright held by the owner/author(s). Publication rights licensed to ACM.

1550-4859/2021/08-ART47 \$15.00

<https://doi.org/10.1145/3461840>

## 1 INTRODUCTION

The road **crowdedness level (CL)**, as a simplified indicator of traffic speed on road segments, has very important applications in urban areas, e.g., real-time routing [7, 15] and emergency response [20]. In particular, Google Maps [17] and Gaode Maps [16] (i.e., a major online map service provider in China) use different colors to imply different CLs on maps, which reflect a travel time delay considering roads speed limits and provide hints for choosing alternative routes to save time. Compared to speed, CL with a low granularity enables a simplified calculation, estimation, and prediction for traffic conditions with a higher sensing and computational efficiency [28, 56].

Due to its importance, CL, or traffic condition in general, has been studied extensively by different sensing systems and their data. For example, vehicular systems and their GPS data [1, 49], loop sensors and their log data [52], cellular networks and their signaling data [10, 23, 32, 54], and even building sensing systems and their occupancy data [55]. In short, the existing CL sensing approaches can be classified into *Explicit Sensing* and *Implicit Sensing* based on their sensing natures. The explicit sensing systems provide direct CL measurements with high accuracy, e.g., vehicular systems and their GPS data as well as loop sensors and their log data. In contrast, implicit sensing systems have indirect CL measurements with low accuracy, e.g., (i) cellular networks and their signaling data, with which CLs are estimated based on changes of cellphone users' attached cell towers along with the associated time interval [23]; (ii) sensing systems for buildings and their occupancy data, with which CLs are inferred based on the learned correlation between building occupancy level and traffic conditions on nearby roads [55].

Even with the above state-of-the-art sensing approaches, real-time urban-scale CL is still challenging to model because of the spatiotemporal coverage and accuracy of sensing systems. For the explicit sensing, its advantage is the accurate measurement, but its spatiotemporal coverage is low due to low penetration rates [38, 40–42]. Moreover, its deployment cost is high due to dedicated purposes [12, 18, 50]. Based on our research results in the Chinese city Hefei, we find that a six-thousand-vehicle network can only cover 28% of the road segments in this city with a one-hour time interval. In contrast, for implicit sensing [10, 22, 23], its advantage is high spatiotemporal coverage due to its high penetration rates [51], but its CL measurement accuracy is low because of indirect measurements [13]. For example, based on our results, we find that the data from cellular networks can only provide 61% accuracy on predicting travel time, since their CL modeling is based on tower-level locations. Besides, implicit sensing usually makes use of existing datasets, which are dedicated to other purposes [8, 30]. To date, it is still unclear which sensing approaches and their data are better for urban-scale CL modeling under what contexts [35]. For a specific region, explicit sensing with a lower spatiotemporal coverage can provide a higher sensing accuracy but may cover the partial area during the limited time; while implicit sensing with higher spatiotemporal coverage may cover all the areas and time with a lower sensing accuracy. Considering this, sensing results can be accurate due to the contribution of accurate explicit sensing, also with high coverage given the contribution from the implicit sensing. Specifically, in our work, the vehicular sensing working as explicit sensing can provide accurate traffic sensing using the GPS data from vehicles, but only partial road networks are covered by the vehicular networks. The cellular sensing functions as the implicit sensing via the interaction log data from the cellular networks and associated users. It provides higher spatiotemporal coverage, since the cellular networks function in a broad area for almost all the time. Despite the lower traffic sensing accuracy, implicit sensing still provides information in areas that are not covered by explicit sensing. Thus, traffic sensing can be more accurate and with higher coverage via the combination of both sensing sources. Given numerous sensing approaches for CL sensing or traffic modeling in general, in this article, instead of providing another single source based sensing approach, we are interested in the evaluation of

which kinds of sensing systems are better in what scenarios, and how can we utilize their individual strengths to collectively address their individual weaknesses. By leveraging both sensing sources, we can expect a result with higher coverage and accuracy.

To achieve this goal, we design a measurement framework called **EXIMIUS** (meaning excellent in Latin) to validate **EXplicit and IMplicit solutIOns for Urban Sensing**. In EXIMIUS, we utilize CL as a concrete metric to quantify the advantages and disadvantages of both explicit and implicit sensing. Different from the existing work focusing on either explicit or implicit sensing, EXIMIUS features a comparative study and explores (i) in which contexts (including spatiotemporal and contextual factors) one approach is better than the other, and (ii) how we can combine the strengths of these two approaches to overcome their individual weaknesses. In particular, the contributions of this article are as follows.

- To our knowledge, we conduct the first quantitative investigation on traffic conditions (quantified by CL) sensing approaches from explicit and implicit perspectives by utilizing two large-scale real-world infrastructures to address the tradeoffs of two approaches considering different sensing features. Our study is mainly based on real-world data from more than five thousand vehicles (GPS data), three million cellphones (signaling data), and seven million residents (census data). Such large-scale infrastructures and data enable us to perform a detailed comparative study on explicit and implicit traffic sensing.
- We design a context-aware measurement framework called EXIMIUS based on GPS data from a vehicular system as an example of explicit CL sensing, and signaling data from a cellular network as an example of implicit CL sensing. With these data, we provide some in-depth analytic results about their spatiotemporal coverage and sensing accuracy. We further compare the pros and cons of two state-of-the-art models based on the data in various settings to evaluate the impacts of population density, region functions, road types, and the rush hours on the performance of these two CL sensing methods.
- We implement EXIMIUS with one month of 893-GB vehicular GPS data and cellular signaling data from Chinese city Hefei, along with context data including population data and road network data. To validate the coverage and accuracy of two kinds of data and their resultant models, we utilize navigation data from one of the largest navigation and map service providers in China as the ground truth for evaluation. To our knowledge, this is the first time that such detailed datasets are utilized to implement an urban traffic sensing project.
- Our measurement results reveal the impacts of various contextual information on CL sensing, providing insights on the tradeoffs between spatiotemporal coverage and sensing accuracy for real-world traffic sensing. Based on our results, we provide a detailed discussion of insights for explicit and implicit urban sensing and important lessons learned. Besides, we discuss the generalizability of EXIMIUS by explaining its ability to function in other cities and to include more data sources, such as bicycles, buses, **call detail records (CDR)**, and so on.
- Based on characteristics of explicit and implicit sensing, we provide a solution to improve spatiotemporal coverage and accuracy of traffic sensing by integrating these two kinds of sensing methods based on a truth discovery scheme. Specifically, we formalize the data fusion problem into a constrained optimization problem and solve it by an iterative optimizing fashion.

The rest of the article is organized as follows. Section 2 describes explicit and implicit sensing systems and their associated data. Section 3 introduces two state-of-the-art models for explicit and implicit sensing and proposes a data fusion solution. Section 4 shows our detailed evaluation

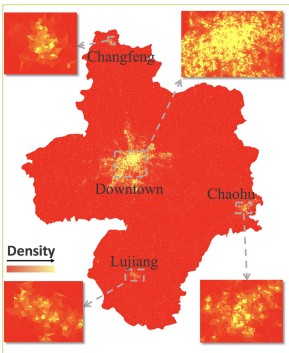


Fig. 1. Voronoi partition.

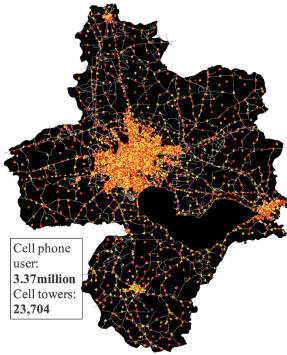


Fig. 2. Roads and cell towers.

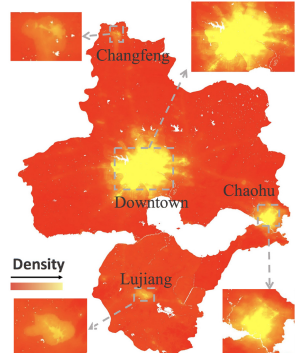


Fig. 3. Population distribution.

results from the individual sensing system and the performance of the data fusion scheme, under different contexts. Section 5 discusses the insights and lessons learned from our comparative analyses. Section 6 provides related work in terms of urban traffic sensing, followed by conclusion in Section 7.

## 2 EXIMIUS: SENSING SYSTEMS AND DATA

To compare implicit and explicit sensing approaches in a fair way, our measurement study focuses on one Chinese city Hefei, i.e., the capital city of Anhui Provence with a total area of 4,372 m<sup>2</sup> and more than seven million population. The two sensing systems we study in EXIMIUS represent two major urban sensing infrastructures from the telecommunication domain [22, 24, 37] and the transportation domain [25, 29, 33, 47, 58]. In Section 2.1 and 2.2, we present these two sensing systems and their sensing data. In Section 2.3, we introduce two contextual data sources and analyze their impacts on CL sensing results. In Section 2.4, we describe how to quantify CLs under different spatiotemporal partitions.

### 2.1 Cellular System for Implicit Sensing

Based on our collaboration, we have access to offline log data from one of the three major cellular operators in China. This cellular operator has deployed 23,704 cell towers in Hefei and provides services for 3.37 million users with 20 GB signaling records generated per day.

**System Granularity:** Based on all cell towers' locations, we implement a Voronoi partition [2] of Hefei as in Figure 1. We find that this cellular network leads to a very detailed partition even on the cell tower level. The distribution of cell region sizes is given in Figure 4. We can see that about 85% of cell regions have a size smaller than 1 km<sup>2</sup> and 5% of regions in the downtown area have a size smaller than 0.01 km<sup>2</sup>, making them fine-grained enough for crowdedness level sensing.

**Data Format:** Signaling data are generated under several protocols, covering events including cell tower attaching, detaching, and cellular data usage, and so on [23]. The detailed format of the signaling record is shown as follows.

- Timestamp: Time when the record was generated at a sub-second level.
- Tower ID: A unique identification of the cell tower from which the record was generated.
- User ID: A unique encrypted identification of the cellphone user associated with this record.
- Web Type: The type of connection the user has established, e.g., 2G, 3G, 4G, or LTE.

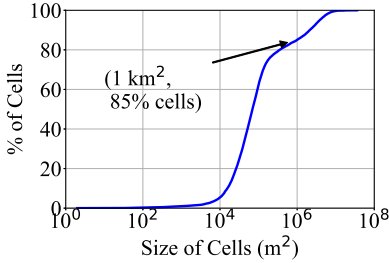


Fig. 4. Cell size distribution.

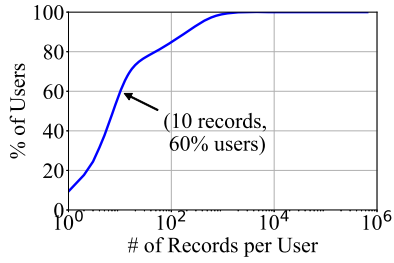


Fig. 5. Record # distribution.

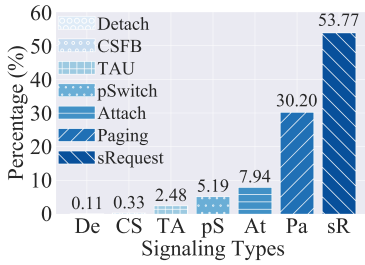


Fig. 6. Record type distribution.

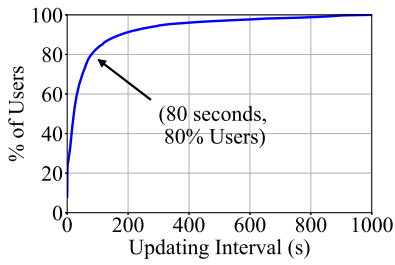


Fig. 7. Updating distribution.

- Service Type: Seven service types in total, including Patch\_Switch, CSFB (Circuit Switched FallBack), TAU (Tracking Area Update), LTE\_ATTACH, LTE\_DETACH, LTE\_PAGING, Service\_Req (e.g., 2G, 3G, 4G, LTE).

**Spatial and Temporal Coverage:** Having the data, we first perform a detailed analysis of signaling data to validate their spatial and temporal coverage for CL modeling.

As shown in Figure 5, we find that 40% of users have more than 10 signaling records per day, providing a large amount of data for urban sensing considering the large number of subscribed cellular users. For all the data generated, we find that more than 50% of signaling data are generated for Service Requests, e.g., phone call, short message service, and Web services, as shown in Figure 6, and a large number of them are for web services, e.g., social network apps, which require frequent data accessing. To further evaluate the data generating frequency, Figure 7 shows the CDF of updating intervals, i.e., the time interval between two consecutive signaling records of one user. We find that 80% of the records have an updating interval shorter than 80 s and the average updating interval is 70.26 s, which indicates a large number of records can be used for CL modeling.

In addition to the temporal aspect, we also analyze the spatial aspect of cellular network data for CL modeling on road segments. Based on location data of towers and roads, we visualize all 23,704 towers in Hefei and Hefei road networks in Figure 2 to qualitatively show the spatial road network coverage of cell towers. Each dot represents one cell tower: A yellow (brighter) dot indicates a higher amount of signaling data records generated in that tower and a red (darker) dot indicates a tower with a lower amount of records. We find that all major road segments' cell towers have a large number of data records, making the CL modeling easier. We also find that the cell towers are distributed densely in the downtown area and sparsely in the suburban and rural areas. There are 48.3% of road segments and 67.9% of towers covering the downtown area (around 6% of the Hefei city area). Besides, we find that almost all downtown road segments are associated with at least one tower, providing convenience for CL inference.

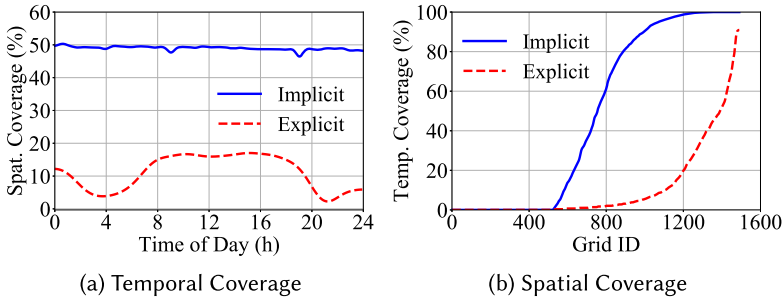


Fig. 8. Spatiotemporal coverage of two sensing systems.

To quantitatively investigate the spatial and temporal coverage of the cellular network and compare it with the vehicular network at the same level, we partition the city into five thousand grids and a day into 288 5-minute slots to analyze the spatiotemporal coverage of two datasets. Figures 8 shows the spatial and temporal coverage rates of the central downtown area, on the grid region level, of 288 5-minute slots upon a day. For the spatial coverage, the  $x$ -axis shows the different time of day and the  $y$ -axis represents the percentage of regions covered by the related sensing data. For the temporal coverage, the  $x$ -axis represents the ID number of the grids, and the  $y$ -axis shows the percentage of 5-minute slots of 288 slots covered by the sensing data. We can see that (i) the spatial coverage of implicit signaling data is generally higher than explicit GPS data during the different time of day, since there are many more cell towers (23,704) and users (three million) in the city than vehicles (4,908) in our datasets. (ii) The spatial coverage of the signaling data is stable during the different time of day, since the region is considered covered once there is cell tower(s) deployed and signaling data are generated, and the region is not covered if there is no cell tower. Besides, the signaling data are generated even when users do not interact with their cellphones, that is the reason why spatial coverage is still high during late night. (iii) For the temporal coverage, we observe that a proportion of the regions are with 0 coverage, it is because there is no cell tower deployed given our fine-grained grid partition. The detailed spatiotemporal coverage makes real-time CL sensing based on the cellular network more complete than the vehicular network.

## 2.2 Vehicular System for Explicit Sensing

Based on our collaboration with an insurance company, we have access to a vehicular network in Hefei with 2,887 private vehicles and 2,021 commercial vehicles, which are used to implement an explicit sensing approach for CL modeling. Due to the operating natures of these two kinds of vehicles, we study them separately as follows.

**Data Format:** With a GPS-level spatial granularity, both private and commercial vehicles are using on-board devices to generate data with the following format.

- **Timestamp:** Time when the record was generated at a level of seconds.
  - **Vehicle ID:** A unique identification of a vehicle, from which the record was generated.
  - **GPS Location:** A set of GPS coordinates indicate the location where the record was generated.
  - **Speed:** A number from 0 to 200 (km/h) indicating the speed of the vehicle when the record was generated.

On average, all private and commercial vehicles upload 1.5 million and 500 thousand records to a central server per day with cellular connection based on their uploading frequency. In Figures 9 and 10, we find that 90% of the private vehicles upload fewer than 1,000 records per day, whereas 80% of the commercial vehicles upload fewer than 300 records per day.

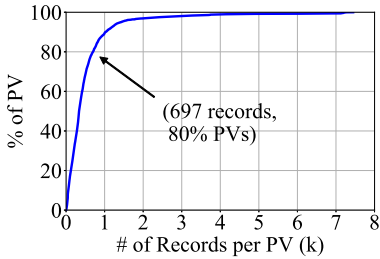


Fig. 9. PV uploading records.

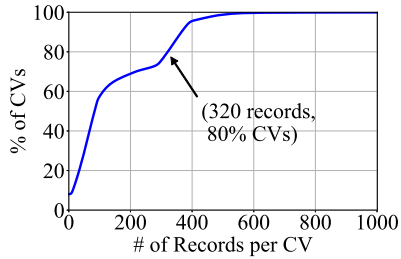
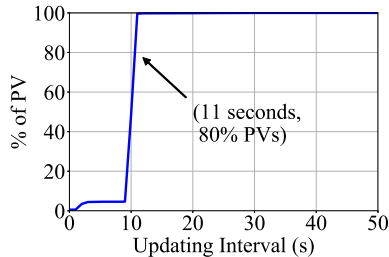
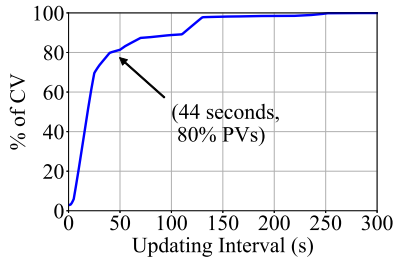


Fig. 10. CV uploading records.



(a) Private Vehicle Interval



(b) Commercial Vehicle Interval

Fig. 11. CDF of vehicular updating interval.

In Figure 11, we further investigate the distribution of updating intervals for these two kinds of vehicles. For the private vehicles, their average updating interval is around 10.17 s; whereas for the commercial vehicles, their average updating interval is around 33.88 s. We can also observe that the updating interval is fixed around 10 s for almost all private vehicles, but changes among different commercial vehicles.

We also qualitatively visualize the distribution of both private and commercial vehicle data on the road map in Figure 12 and 13 with their one-day data, where the yellow (brighter) color indicates a higher vehicular data density and red (darker) color means a lower vehicular data density. We find that most of the road segments can be covered by either one of them. But a daily coverage is too coarse-grained for real-time CL modeling. Specifically, hourly road coverage is only around 27.9% for private vehicles and 13.8% for commercial vehicles. To further evaluate their fine-grained spatial and temporal distributions, we show their spatiotemporal coverage over five thousand regions and 5 min slots in Figure 8. We observe that (i) the spatial coverage of vehicular network has a clear diurnal pattern, since the majority of the drivers rest during the night and become active during the day; (ii) fewer regions and less time of day are covered by the vehicular network compared to the cellular network. Thus, under such a fine-grained spatial and temporal granularity, coverage of explicit data is low, which makes it challenging for them to model CL in real time at the city scale.

### 2.3 Contexts

To contextualize our CL modeling, we utilize two kinds of context data: (i) population, i.e., WorldPop data [39]; (ii) road networks, i.e., OpenStreetMap data [19].

**WorldPop Data:** WorldPop dataset is an open population dataset [39], which provides the static population with a spatial granularity of 100 m × 100 m by fusing multiple data sources including survey data, satellite picture data, and so on. We visualize the population of Hefei city in Figure 3,

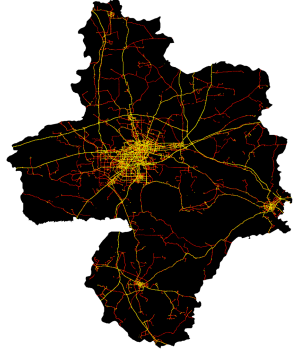


Fig. 12. Private vehicle dist.

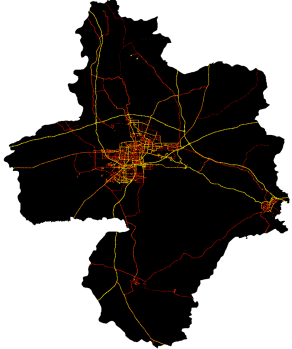


Fig. 13. Commercial vehicle dist.

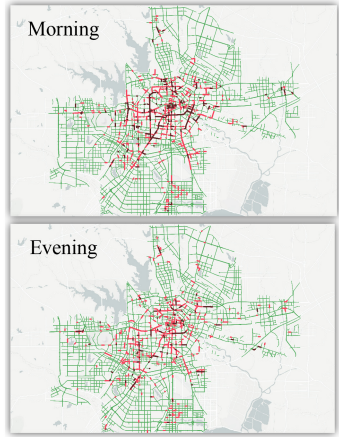


Fig. 14. Ground-truth data.

where the color yellow represents a high population density. We find that most of the residents are living in the downtown area. Such a detailed dataset provides a valuable urban density context for us to understand the performance of implicit and explicit sensing approaches. The total population calculated by WorldPop data is 7.1 million, close to the population released by the Hefei city government.

**OpenStreetMap Data:** OpenStreetMap data [19] provide us with detailed roads and POI (i.e., points of interest) information in our target city Hefei. In the OpenStreetMap data, each road segment is assigned with one of eight types, i.e., Motorway, Trunk, Primary, Secondary, Tertiary, Residential, Unclassified, and Special. Figure 15 shows the road types distribution in Hefei, and we find that 81.8 % of road segments are Motorway, Trunk, Primary, Secondary, Tertiary, and Residential, which can be covered by vehicular data we have. With the data from OpenStreetMap, we aim to understand the impact of different road types on the performance of two sensing systems.

#### 2.4 Metrics: Crowdedness Level

In this article, we utilize the CL to quantify the final results from these two kinds of sensing approaches. The CL has been widely used in the online map services [17] and transportation community [31, 53]. Formally, the CL is associated with a spatiotemporal combination, e.g., a 5-minute time slot and a road segment, and is quantified by a ratio of the extended travel time on this road segment for this particular time to the shortest travel time during any time slot. Essentially, a bigger CL value indicates a longer travel time or a heavier traffic jam on the road segment.

**Spatial Partition:** From the spatial perspective, we study CL on two different levels: one is the road segment level where all road segments are obtained by OpenStreetMap data; another is the Voronoi region level where all regions are defined by the Voronoi graph. The road segment level CL works better for explicit vehicular sensing where we infer travel time on road segments and obtain CL directly; whereas the Voronoi level CL works better for implicit cellular sensing where we perform a more complicated inference process. In detail, we first find regions with at least one road segment within them (e.g., all Voronoi regions in the downtown have at least one road segment). For the region with multiple road segments, we then calculate a comprehensive CL by taking all road segments within this region into consideration and put weights on them according to the length of the road segment in this region. Compared to traditional spatial partition without

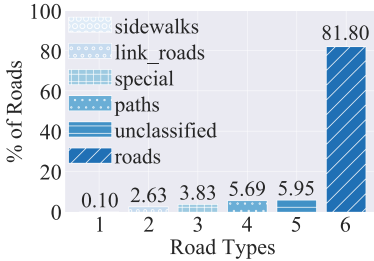


Fig. 15. Road type dist.

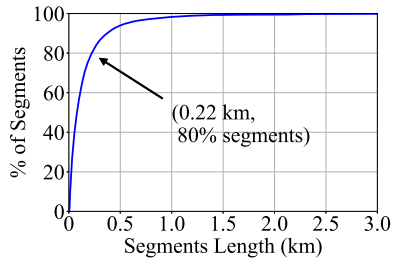


Fig. 16. Segment lengths.

logical contexts, such as straightforward grid partition, our context-aware partition enables a more balanced spatial unit for CL modeling [43].

**Temporal Partition:** Considering the previous work [3] and the fact that 5-minute time slot is the finest temporal granularity we can have, due to updating frequency of the ground-truth data we introduce later, we evaluate different time slot lengths, i.e., 5, 10, and 20 minutes, in practical settings to test the performance of explicit sensing and implicit sensing on different temporal granularity. Further, to put our inference into a general context, we also consider the time of day as a factor to evaluate their impacts on CL inference.

## 2.5 Ground Truth

For the evaluation purpose only, we have obtained dataset from one of the biggest navigation service companies in China as ground truth, which are independent of the explicit and implicit data. It provides real-time information about the crowdedness level of 47% of the road segments in the city, covering the entire downtown area of the city. Their real-time CL data are obtained by a high-cost proprietary solution based on data sources including traffic cameras, loop sensors, floating vehicles, and so on. There are four different CL values ranging from 1 to 4, denoting an increasing traffic jam. Such detailed real-time CL data are very challenging to obtain at a large scale due to the difficulty of extensive sensing infrastructures deployment [3]. We visualize all the road segments with the ground-truth data in Figure 14 with four colors and we find that the ground-truth data only cover the downtown area. During the evening rush hour from 8:00 to 9:00 pm, we have 89.0%, 8.7%, 1.5%, and 0.3% of road segments for four crowdedness levels, respectively. The lengths of different road segments are shown in Figure 16, from which we find that almost 95% of road segments have a length of shorter than 0.5 km, enabling a fine-grained CL modeling.

## 3 EXIMIUS: DATA-DRIVEN MODELS

The overall framework of EXMIUS is demonstrated in Figure 17. Since our measurement framework EXMIUS focuses more on evaluating two kinds of urban sensing approaches (Section 3.1 and Section 3.2), instead of designing a new sensing scheme, we first utilize the sensing infrastructure and their data introduced in the last section to implement two state-of-the-art models regarding single source traffic sensing, then we propose a data fusion method based on truth discovery to consider both sensing sources (Section 3.3). All the evaluations (Section 4) are performed on both explicit and implicit sensing sources and evaluated based on the ground truth introduced in Section 2.5.

### 3.1 Model Driven by Implicit Sensing Data

Among several state-of-the-art models for CL modeling (traffic condition modeling in general), we utilize the model from Reference [23], which is the latest model using detailed cellular signaling

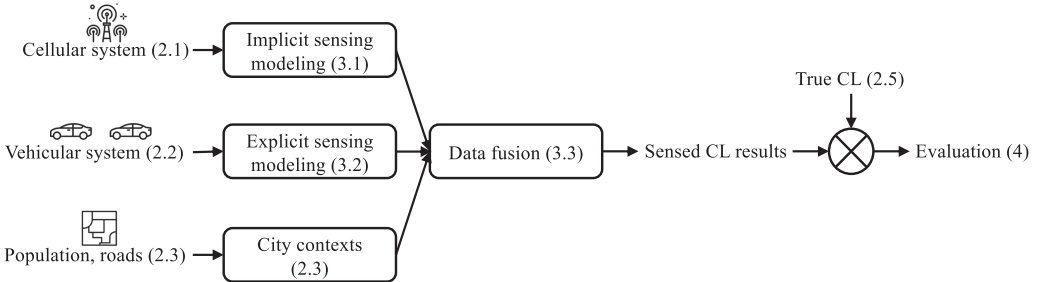


Fig. 17. Overall framework of EXIMIUS.



Fig. 18. GPS and signaling trace of a user.

Table 1. Comparison of CL Estimation

Data	Ave. speed	Speed variance	Travel time	Ref. speed
GPS	10.0 (m/s)	33.6	669.0 (s)	8.84 (m/s)
Signaling	100.1 (m/s)	18671.51	690.0 (s)	8.84 (m/s)

data for travel time and crowdedness level inference. However, since this is a data-driven model, we utilize a few techniques to ensure our cellular signaling data can be used to implement this model.

Intuitively, the travel time can be extracted by simply considering two signaling records from two different cell towers. We show a test trace of a user with both GPS data and signaling data in Figure 18.

The left figure visualizes the raw GPS data and the right figure presents the trace of attached cell towers. We find that two traces have high-level similarity, but the trace based on signaling data is more uncertain. In particular, consider the fact that the length of most road segments in Hefei road networks is shorter than 0.5 km (Figure 16), and the coverage radius of a cell tower is roughly 300 m, it is challenging for us to estimate travel time on the road segment level by using signaling data. This is because the coverage distance between cell towers can be as long as 600 m, which is even greater than the length of road segments. This leads to large estimation error considering that a cellphone user standing on the border of two cell towers can be attached to either tower at any time due to the congestion control of the cellular networks, leading to the phenomenon called “Ping-Pong Effect” [21], meaning a cellphone user quickly “moves” between two cell towers.

To better validate the claims above, we analyze some statistic features from the traces of GPS and signaling data of this one user and present the results in Table 1. The Ref. speed is the reference average speed calculated by real physical trace distance (5.9 km) and absolute travel time (691 s).

We find that the speed calculation based on signaling data cause larger error compared to GPS data, but travel time is relatively accurate. Besides, it is not reasonable to calculate travel time between short distances, especially for a distance shorter than the coverage radius of one tower,

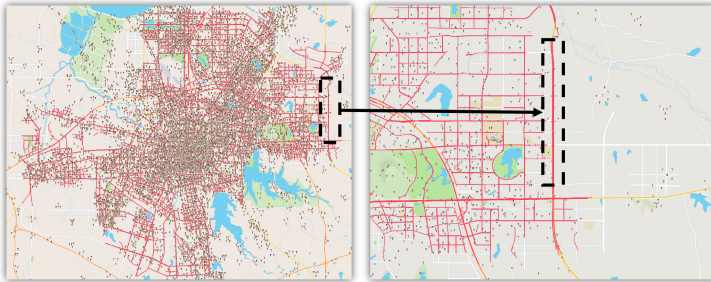


Fig. 19. Example of a highway segment.

**ALGORITHM 1:** Algorithm of selecting cell tower pairs

---

```

 $t_{max}$   $\Leftarrow$  maximum travel time of target road segment
 $t_{min}$   $\Leftarrow$  minimum travel time of target road segment
 $dist_{max}$   $\Leftarrow$  maximum distance of two cell towers
 $dist_{min}$   $\Leftarrow$  minimum distance of two cell towers
 $T$   $\Leftarrow$  set of cell towers in proximity of target road
for  $tower_i$  in  $T$  do
    for  $tower_j$  in  $T$  do
        if  $i \neq j$  and  $dis_{min} \leq distance(tower_i, tower_j) \leq dis_{max}$  and  $t_{min} \leq$ 
         $time(tower_i, tower_j) \leq t_{max}$  then
            Calculate direction of cell tower pairs
            Calculate travel time of cell tower pairs
        end if
    end for
end for
Return cell tower pairs satisfying all conditions

```

---

since it will be challenging either to distinguish the moving status of a cellphone user or to estimate the travel time precisely. Thus, we choose relatively longer real-world road segments as our target roads and implement the algorithm in Reference [23] with extra constraints.

Based on Algorithm 1, we first extract candidate cell tower pairs where each cell tower in a pair is near one end of the road segment. Cell tower pairs are selected by thresholds of coverage radius of cell towers and distance within cell tower pairs, i.e., cell towers must be near the ends of the road segment and the distance of two cell towers must not be larger than the threshold regarding road segment length. After this, we then select users who were attached to the cell tower pairs by setting travel time and travel distance thresholds, then we can have all the target users associated with cell pairs traveling in two driving directions on the target road segment. Actually, we find that setting limits for the distance of cell tower pairs alone is enough for filtering the outliers of towers and users. Note that for a specific user, there may be multiple records, so we implement an intuitive algorithm for the final travel time calculation [23]. The main idea is to consider (i) the time of the last signaling record attached to the departure cell tower as the starting time, (ii) the time of the first signaling record attached to the arrival cell tower as the ending time, and (iii) the average travel time for different users as the final travel time on the road segment.

We utilize a highway segment given in Figure 19 called national highway G206 to show an example of how to calculate the travel time based on signaling data [23]. This segment of national

highway G206 has a total length of 8.2 km and the maximum speed for the road is 120 km/h (i.e., corresponding to a travel time of 4.2 minutes). There are 235 towers in proximity and 1,618 different road segments on this road, and 9,153 users during a day recorded by signaling log. The maximum number of records for a single user is 2,252; the minimum number is 2; the average number is 40. Based on the travel time calculation algorithm, we can first find out candidate cell tower pairs, then we select attached users traveling from two directions during a different time of day to calculate their travel time intervals on this road segment. Last, we convert the resultant travel time into the CL based on different speed ranges of four CLs and the road segment length.

The accuracy of indirectly inferring travel time may not be very high, since we cannot have the precise position of the users. However, the advantages of this implicit sensing method can be manifold: (i) it utilizes the ubiquity of cellphones and telecommunication infrastructures, which are free for the traffic sensing purpose; (ii) it also makes full use of the advantages of crowdsourcing, i.e., in our scenario, the large scale of subscribed cellphone users can make up for the weakness of sensing accuracy.

### 3.2 Model Driven by Explicit Sensing Data

Based on the explicit sensing data, we implement a travel time estimation model to obtain CLs for all road segments with different time intervals. Given the historical GPS data we have and the features of these data, we implement the model from Reference [3] as our explicit sensing model, where an algorithm focusing on creating a prediction multidimensional tensor by referring to historical GPS data at the same region partitioned and similar time is introduced. Even though some models are proposed recently [52], they either require additional datasets or their model descriptions are at a high level, and cannot be implemented with details for a fair comparison.

During the implementation of our explicit sensing model, we utilize a spatial partition based on Voronoi polygons generated by locations of cell towers to provide a fair comparison with signaling data. As for the temporal aspect, we still consider a similar partition, i.e., time of day. Inputs of the model are raw GPS data from private vehicles and commercial vehicles. They are formatted into traces by different users and different periods. Different from storing historical travel duration into entries, we store crowdedness level into entries for two reasons: (i) we directly compare CL derived from signaling data in the end, so it would be more efficient for us to store CL directly; (ii) it is challenging to calculate travel duration given specific boundaries of polygon regions, since the segmentation of trips is needed. However, after converting travel time to the corresponding CL, we can easily obtain CL results by examining how the CL calculated by this trip contributes to the actual overall CL of the corresponding roads.

Note that we do not average all the historical data directly, instead, we consider the values of different CL within the specific time and location to improve the accuracy in our case. The detailed are given in Algorithm 2 [3].

The advantage of explicit sensing is clear, since it provides us with accurate and frequently updated location information. High-quality GPS data can be used for traffic sensing such as travel time estimation with little preprocessing work. However, the spatiotemporal coverage of the data cannot be guaranteed, since it is decided by the appearance of vehicles with GPS modules.

### 3.3 Data Fusion based on Truth Discovery

Once we have obtained the estimated CL results from explicit and implicit sensing methods introduced above, we then try to approach the “true” CL data on the road segments and regions based on both sensing sources. Due to the distinctive spatiotemporal coverage advantage of implicit sensing and the accuracy advantage of explicit sensing, we try to make use of the advantages from both to provide a better sensing performance. To achieve that, we formulate this problem into a

**ALGORITHM 2:** Algorithm of travel time estimation

---

```

 $T \Leftarrow$  All traces of users
 $P \Leftarrow$  All Voronoi polygons
 $M \Leftarrow$  Matrix storing historical CL data
 $m_{pt} \Leftarrow$  CL of time period  $t$  and polygon region  $p$ 
for trace in  $T$  do
    Convert travel time to CL
    if  $m_{pt}$  does not exist then
        Create an entry under this context
        Assign value of CL to the entry
    else  $m_{pt}$  exists
        Append value of current CL to  $m_{pt}$ 
    end if
end for
Update  $M$  with weighted entries
return  $M$ 

```

---

truth discovery problem [27] in this work. As indicated, truth discovery works well in the scenario where there are conflicts from multiple data sources, which is quite common in real-world sensing scenarios. Specifically, in our scenario, we treat the ground-truth CL on road segments and regions as the “truth” we are seeking, the estimated CL results from two sensing sources are regarded as observations upon the truth. The goal here is to discover the truth from multiple sources.

To begin with, we formulate the problem in a general way by defining  $\mathbf{x}_t^*$  as the truth of CL under certain spatiotemporal context, i.e., on a road segment during time  $t$ ;  $N$  as the number of views we consider;  $\mathbf{x}_t^n$  as the CL result derived from the single-view models we introduced above,  $\mathbf{w}_t^n$  as the explicitness degree regarding a view  $n$ . The explicitness degree represents how explicit the sensing source is, for example, in our traffic sensing scenarios, the vehicular GPS sensing data should have a higher  $\mathbf{w}_t^n$  value, since it is more explicit in terms of sensing traffic condition. We also define  $\mathbf{W}_t$  as the vector of  $\mathbf{w}^n$ :  $\mathbf{W}_t = (\mathbf{w}_t^1, \dots, \mathbf{w}_t^N)$ . Based on these, we then use a loss function  $D$  to measure the deviation from the true CL  $\mathbf{x}_t^*$  to the observed CL  $\mathbf{x}_t^n$  from sensing source  $n$ , and a regularization function  $\delta$  to constrain the explicitness degrees. In sum, the problem can be formulated as a joint optimization problem to obtain  $\mathbf{x}_t^*$  and  $\mathbf{W}_t$  in Equation (1):

$$\begin{aligned} \min F(\mathbf{x}_t^*, \mathbf{W}_t) &= \sum_{n=1}^N [\mathbf{w}_t^n \cdot D(\mathbf{x}_t^*, \mathbf{x}_t^n)], \\ \text{s.t. } &\delta(\mathbf{W}_t) = 1. \end{aligned} \quad (1)$$

The object function we try to minimize, i.e.,  $\sum_{n=1}^N [\mathbf{w}_t^n \cdot D(\mathbf{x}_t^*, \mathbf{x}_t^n)]$ , is the overall weighted deviation covering different views, in which a higher penalty will be given if the CL from a more explicit view deviates from the true values and a lower penalty will be given if the CL of a less explicit view deviates from the truth. That means, we put more weight on the observations from the explicit view and the penalty will be high if the observations are far away from the true values.

Given this formulated optimization problem, we further use the block coordinate descent method [5] to obtain the optimized  $\mathbf{x}_t^*$  and  $\mathbf{W}_t$  to minimize the object function. The method can be described as iterative processing where one unknown variable is fixed and the other is optimized, then we do it in the other way. Specifically, we initialize the  $\mathbf{x}_t^*$  and  $\mathbf{W}_t$  in the step 0. In our setting, the  $\mathbf{x}_t^*$  is initialized as the average from multiple sensing views and  $\mathbf{W}_t$  is set as a vector of equal values constrained by the regularization function. Then we fix  $\mathbf{x}_t^*$  to optimize  $\mathbf{W}_t$  as the step 1, and

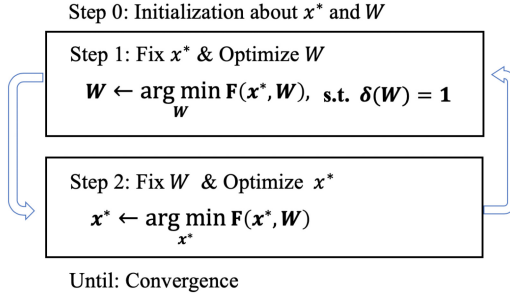


Fig. 20. Optimization processing.

fix  $\mathbf{W}_t$  to optimize  $\mathbf{x}_t^*$  as the step 2. We iteratively repeat step 1 and step 2 until the results are converged, as shown in Figure 20.

The only unsolved parts are the choices of the loss function and regularization function. In this joint optimization problem, we use the normalized squared loss as loss function and negative log function as regularization function, which makes the optimization convex. The convergence of this problem is guaranteed by the property of Block Coordinate Descent method [5]. In detail, the two functions are given in Equation (2) and (3):

$$D(\mathbf{x}_t^*, \mathbf{x}_t^k) = \frac{(\mathbf{x}_t^* - \mathbf{x}_t^k)^2}{std(\mathbf{x}_t^1, \dots, \mathbf{x}_t^n)}, \quad (2)$$

$$\delta(\mathbf{W}_t) = \sum_{n=1}^N \exp(-\mathbf{w}_t^n). \quad (3)$$

The deviation function first calculates the L2 distance from the true values and the observed values, then it is normalized by the standard deviation of all the observations. In this way, we can have a fair representation of the deviation from observed values and the true values. For the regularization function, we use the exponent function to magnify the subtlety of the explicitness degree. There are other realizations of the loss function and regularization function that can guarantee the convexity of the optimization problem, here we only show one kind of realization to demonstrate the feasibility.

## 4 EVALUATION RESULTS

In this section, we show our evaluation results from CL modeling in Section 3. To comprehensively compare these two kinds of sensing approaches, we first introduce the methodology of evaluation (Section 4.1), then we consider several factors affecting the performance of traffic sensing, i.e., evaluation sites (Section 4.2), spatial impacts (Section 4.3), temporal impacts (Section 4.4), and impacts from various contextual information (Section 4.5). Then we show the performance of the data fusion method based on both sensing systems (Section 4.6).

### 4.1 Evaluation Methodology

In general, the evaluation results will be introduced from two levels. One level is the estimation and the other level is the prediction. We want to investigate how different factors can affect the performance of both estimation and prediction.

For the estimation (sensing part), we directly implement three sensing models (explicit, implicit, and fusion model) introduced in Section 3. Inputs of these models are based on the raw data from two sensing systems, we treat the process of sensing as the estimation. The second level is the

Table 2. Statistics of Road Segments

Context	Road 1	Road 2	Road 3	Road 4
Road type	avenue	main ave.	motorway	highway
Road len.(km)	2.23	1.9	0.9	2.6
# of segment	1595	395	1709	2782
# of GPS users	273	509	680	710
# of GPS recs	14,921	11,342	65,314	81,100
# of towers	403	365	804	1017
# of tele users	76,615	92,976	240,549	246,324
# of tele recs	3,504,747	4,126,435	10,429,728	10,723,447

prediction. The details of data preprocessing and model implementation will be shown in the corresponding paragraphs below. Consider the massive data size, all the data processing work is done on a cluster with 12 Hewlett-Packard machines, with 2 Tesla K80c on each. We use Spark on the cluster for initial data preprocessing such as outlier filtering, data aggregation, and so on. Further sensing models are implemented on the same cluster.

Once we have the estimated CL results from different models, i.e., CL from the explicit model, implicit model, and fusion model, we then build models on the historical data to predict future results. Here we implement a **Multi-layer Perceptron (MLP)** based time series model to predict future CL results. Notice that MLP here is only used as an example method to demonstrate the effectiveness and generalizability of our framework; other time series methods should also work. For the MLP model, we split the time series of CL values into short time sequences, where each sequence has a length of five. We then use the previous four values to predict the next value. Specifically, we design a three-layer MLP structure with a hidden regular densely-connected layer of 100 nodes. We use the Rectified Linear Unit as activation function, *Adam* as optimizer, and *MSE* as the loss function. The model is implemented via *Tensorflow*. We sample 80% of the data as training and the rest 20% of the data as testing data.

All the performances, including estimation and estimation, are quantified by one metric: **Mean Absolute Percentage Error (MAPE)** (shown in Equation (4)). The  $CL_{inferred}$  can be estimated or predicted CL values, and the  $CL_{true}$  can be the ground-truth CL from the navigation company if it is for estimation or the estimated results if it is for prediction. The lower the MAPE value, the higher the accuracy,

$$MAPE(\%) = \frac{|CL_{inferred} - CL_{true}|}{CL_{true}}. \quad (4)$$

## 4.2 Comparisons on Four Evaluation Sites

Since different road types typically have different speed limits and traffic volume capacities, we perform a data-driven investigation of four kinds of road types based on Hefei road networks. We report our statistic results in detail based on four roads from four kinds of these road types. These four roads have different road lengths from 0.9 to 2.6 km, and have a different number of road segments from 395 to 2,782, and are from different urban regions around the city, i.e., commercial area, residential area, industrial area, and airport highway area. By considering all these possible features regarding road segments we can make sure our evaluation sites are representative. The average statistical characteristics from these four roads are given in Table 2.

To compare cellphone-based explicit sensing and vehicle-based implicit sensing, we combine private vehicles GPS data and commercial vehicles GPS data together as vehicular data to implement the explicit CL sensing model described in Section 3.2. We compare this model with the

Table 3. Comparison of CL Estimation

Context	Road1	Road2	Road3	Road4
Accuracy (Explicit) (%)	98.6	97.2	98.6	98.6
Coverage (Explicit) (%)	44.4	45.8	45.8	86.1
Accuracy (Implicit) (%)	61.1	73.6	62.5	73.6
Coverage (Implicit) (%)	100	100	100	100
Explicit CL var.	0.52	0.31	0.26	0.08
Implicit CL var.	0.22	0.03	0.04	0.16
Ground Truth CL var.	0.17	0.18	0.22	0.05

implicit CL sensing model based on the telecommunication data, i.e., signaling data, as described in Section 3.1. From the Table 2, we find that in our dataset, the implicit sensing data, i.e., signaling data, have many more records and users logged during a day compared to the explicit sensing data, i.e., vehicle GPS data. One reason is that we have many more cellphone users than car users; another reason is that signaling data update much more frequently, leading to a higher temporal coverage rate. With these data, we calculate the results of the CL inference of these four sample roads and then compare them with the ground-truth data introduced in Section 2.5. The detailed estimation results are summarized in Table 3.

From the above results, we find that with a 5-minute time slot length setting, the temporal coverage rate of vehicle-based explicit sensing is lower than that of cellphone-based implicit sensing across all evaluation road segments. Even though their overall temporal coverage rates are smaller than these of implicit sensing data, explicit sensing data enable a sensing approach with better accuracy, which verifies our previous observation that cellphone-based implicit sensing has better coverage, but vehicle-based explicit sensing has higher accuracy. Further, by calculating the CL variance, we find that a smaller variance normally corresponds to a higher estimation accuracy in both cellphone-based implicit sensing and vehicle-based explicit sensing for the CL estimation.

### 4.3 Spatial Factors

Traffic sensing is also heavily affected by the following spatial factors: (i) urban region functions, e.g., the downtown area may be more crowded and thus traffic may be heavier, and a rural area may be less crowded; (ii) road lengths, e.g., the longer road may contain more vehicles and more cellphone users to contribute to the sensing; (iii) road types, e.g., the highway may have less traffic jam compared to other road types. Thus, we further explore the impacts of spatial contextual information on two sensing approaches.

Based on Figure 21, the CL prediction results from both sensing approaches indicate that highway has a higher prediction accuracy than other road types, e.g., Road 4 has the best performance. Further, the road length may have a big impact on the prediction results, since the shortest Road 3 has the biggest MAPE value compared to other roads. For all results, it seems that the MAPE value is inversely proportional to road lengths, indicating that the CL prediction on a shorter road segment may cause larger errors. This is because there are fewer data points when the road is shorter, sparse data points may bring biases, since they cannot accurately reflect the real traffic status of road segments. Finally, the cellphone-based implicit sensing has a lower CL prediction accuracy in general compared to vehicle-based explicit sensing except for the highway, which contains enough signaling data across cell towers to estimate CLs.

In addition to road-based setting, we also implement a region-based CL prediction for these two approaches based on Voronoi regions. For cellphone-based implicit sensing, we calculate user density and population density from Worldpop data in each region for later analysis of contextual

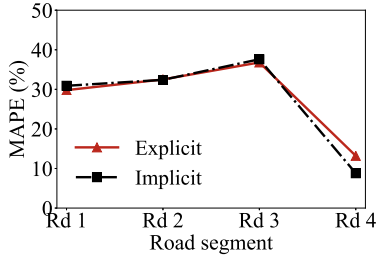


Fig. 21. Road accuracy.

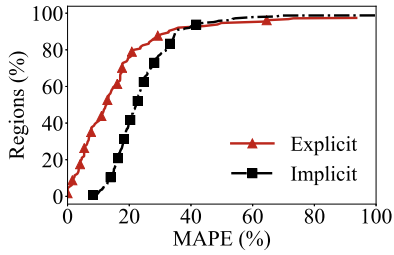


Fig. 22. Region accuracy.

factors. We also consider CLs inferred by users' switching between different towers, and then implement prediction by the MLP model mentioned in the beginning. For the inference of CL based on users, we first filter users with the higher radius of gyration [4] values, then we extract signaling traces from these users as raw traces. Based on these raw traces, we implement the trajectory segmentation method in References [14] to divide the user's one-day signaling trace into several physical trajectories. Then, we smooth the trajectories by excluding spatial outliers caused by handover protocols and "Ping-Pong Effect." Finally, we calculate travel time and travel speed based on individual users, then assign the CL into Voronoi regions according to the location of the users.

For vehicle-based explicit sensing, we implement a state-of-the-art model [3] by first partitioning the whole city into five thousand grids and then locating Voronoi regions in these grids, saving time to locate the entries of each GPS point for the later prediction. Once we obtain a user's location, we first locate it in large grid partitions and then locate its associated Voronoi polygon. Finally, we store each user's speed and timestamp as an entry into the matrix. Estimation results from two data sources are shown in Figure 22 based on a 5-minute time slot temporal partition. Based on the results, we find that for region-based CL sensing, vehicle-based explicit sensing still outperforms cellphone-based implicit sensing, which is consistent with our previous observation.

#### 4.4 Temporal Factors

Different time of day can directly affect the traffic status, e.g., traffic will be more crowded during the rush hours. Since the CLs of the rush hours are more important due to the potential higher traffic demand, we mainly study the temporal contexts during six hours, i.e., 6–7, 7–8, and 8–9 in the morning representing the morning rush hours; 16–17, 17–18, and 18–19 in the afternoon representing the evening rush hours. The time slot length, as another temporal factor, is also vital to our traffic sensing performance. We use 5, 10, and 20 minutes of time slots to test their performance on different temporal granularity. In all, we show the CL prediction performance at both different time of day, and in different time slots.

Based on our previous Voronoi region partition, we investigate the traffic CL prediction based on Voronoi regions by randomly selecting 1,000 regions in Hefei downtown area where Ground Truth data are available, with their specific features on the Voronoi polygon size, the number of cellphone users, and the number of population from Worldpop data. In particular, we use 80% of a one-month CL dataset as training data and 20% of them as testing data; and after rotating the test data among 30 days, the average results were reported.

In Figure 23, we show estimation MAPE of the 1,000 regions from the downtown area during morning and evening rush hours in 5-minute slots, based on historical CL data. We find that the MAPE values are similar in these six rush hours. Further, 08h00 and 18h00 have higher MAPE compared to the other four rush hours, respectively. These results match the trend of CL during

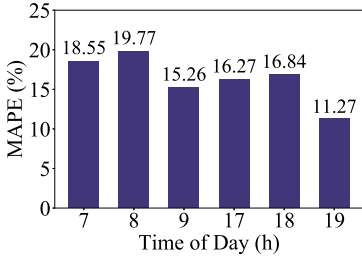


Fig. 23. CL prediction.

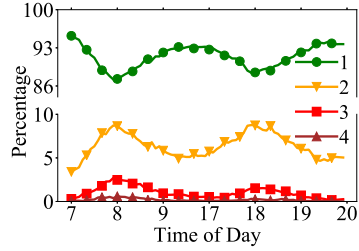


Fig. 24. Gaode CL dist.

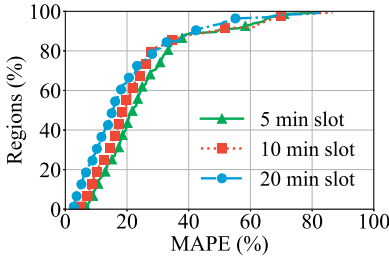


Fig. 25. Temp. of phone.

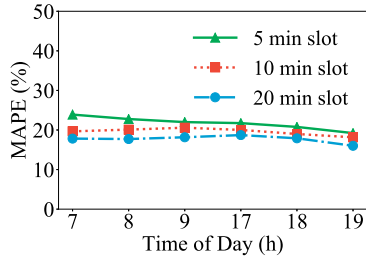


Fig. 26. 6 Hour of phone.

a day in Figure 24 (where 1 means no traffic jam and 4 denotes heavy traffic jam), showing that these two hours are the most crowded periods in one day. We calculate the variance of Ground Truth CL of 6 hours in the same regions, and we find that these two hours have a relatively higher variance than the other four hours. As a result, a lower fluctuation may provide a better estimation of the CLs due to better sensing.

For cellphone-based implicit sensing, we show the impacts of different time slot lengths on the CL prediction results in Figure 25. We find that as we increase the length of the time slot from 5 to 20 minutes, MAPE generally decreases. This is because the CL in a longer time slot, e.g., 20 minutes, is easier to predict due to less fluctuation and more data collected compared to the CL in a shorter time slot, e.g., 5 minutes. Further, we explore the CL prediction results during the different time of day in Figure 26. In particular, we average the accuracy within an hour based on different time slot lengths. We find that a longer time slot can lead to a lower MAPE, i.e., a higher prediction accuracy.

For vehicle-based explicit sensing, we show the impact of different time slot lengths on the CL prediction results in Figure 27 and the impact of time of day on CL prediction results in Figure 28. We find some similar trends as results from cellphone-based implicit sensing. In particular, a relatively long time slot leads to a smaller MAPE value, i.e., higher CL prediction accuracy. Similarly, 8h00 and 18h00 have relatively lower prediction accuracy, matching the results from cellphone-based implicit sensing due to high traffic demand.

Finally, we compare the results of vehicle-based explicit sensing and cellphone-based implicit sensing. We find that as shown by Figure 25 and Figure 27, given the same temporal granularity, i.e., the same time slot length, vehicle-based explicit sensing has a lower MAPE (i.e., higher accuracy). Similarly, as shown by Figure 26 and Figure 28, we find for the same time of day, vehicle-based explicit sensing has a lower MAPE compared to cellphone-based implicit sensing. The above results indicate that given the same time of day and the same time slot length, vehicle-based explicit sensing has better performance in terms of CL prediction than cellphone-based implicit sensing.

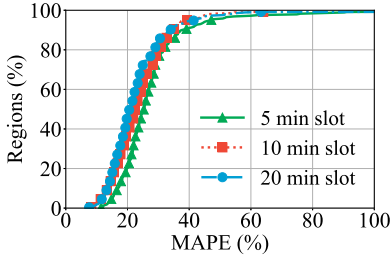


Fig. 27. Temp. of vehicle.

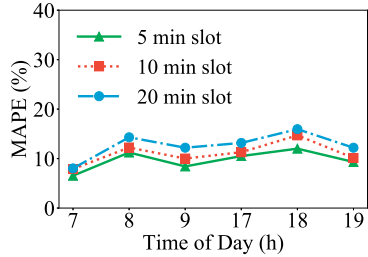


Fig. 28. 6 Hour of vehicle.

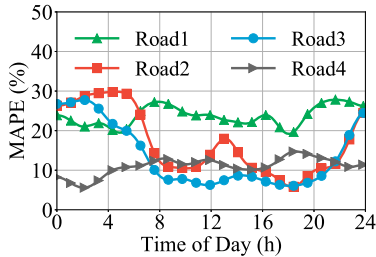


Fig. 29. Temp. of implicit.

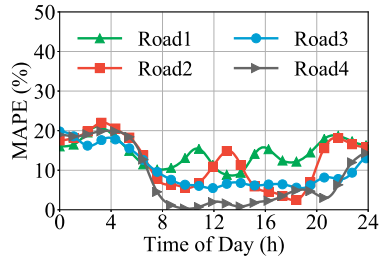


Fig. 30. Temp. of explicit.

Besides, we also show estimation results from non-rush hours upon our four sample roads by implicit sensing (Figure 29) and explicit sensing (Figure 30), compared to the ground truth data from the navigation service provider. We find that generally, explicit sensing has better performance than implicit sensing, and Road 4 (highway) has a smaller estimation error. One possible explanation is that for the non-rush hour, the implicit sensing is only based on limited cellphone data, which leads to poorer performance.

#### 4.5 Contextual Factors

Traffic sensing may also be influenced by other contextual factors, such as region size, population density, and user density, e.g., more users may indicate a higher traffic volume. We show how the contextual information influences the final inference result, aiming to provide insights into how to improve CL inference accuracy. Based on the Voronoi regions, we present our prediction results from ascending sorted polygon sizes, population density, and user density. The results are in Figures 31, 32, and 33, respectively. It is shown in Figure 31 that MAPE decreases as regions' sizes increase, which indicates larger regions can have better CL prediction accuracy, it is because larger regions include more road segments. We find that the MAPE increases (i.e., CL prediction accuracy decreases) if there are a higher population or more users in the polygon, as indicated by Figure 32 and 33.

Last, we comprehensively demonstrate the effects of the common contextual factors on traffic sensing, including weather, day of the week, holidays, and so on. For the weather conditions, we extract the historical weather conditions data online, including daily temperature range, air quality ratings, weather conditions, and wind information. Regarding traffic sensing, we focus on factors that may affect the urban traffic, i.e., factors related to extreme weather conditions, including heavy rain or above, wind scale 6 or above, and heavy air pollution. For the day of the week, we separate days into weekdays and weekends. We also evaluate the impacts of holidays, e.g., the traffic is usually heavy near International Workers' Day. For these above factors, we compare the performance of traffic sensing on days with and without these characteristics. The results are shown in

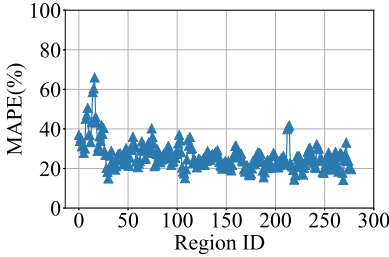


Fig. 31. Polygon size.

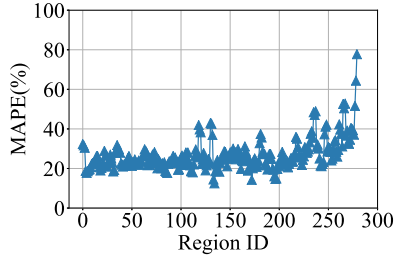


Fig. 32. Population.

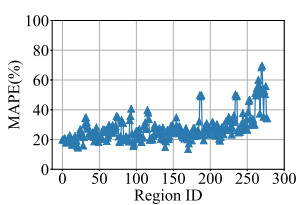


Fig. 33. User number.

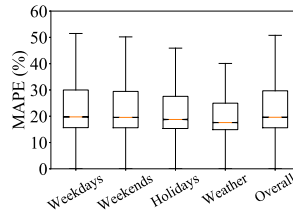


Fig. 34. Other contexts.

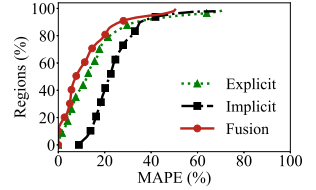


Fig. 35. Performance comparison.

Figure 34. We can observe that the MAPE values of weekends are slightly smaller than those of weekdays, indicating a higher sensing accuracy during weekends. This may be caused by fewer people going out during weekends compared to weekdays, e.g., some people tend to rest at home while they have to work during weekdays. We also find out that the performance of traffic sensing during holidays and under extreme weather conditions is better than regular days, which suggests a better sensing accuracy. For example, the traveling speed may be slower but more stable during a day with heavy rain, which makes sensing easier.

#### 4.6 Data Fusion based on Truth Discovery

Upon having the sensed CL from explicit and implicit sensing sources, we implement the data fusion method introduced in Section 3. Considering that we can infer CL by either cellphone-based implicit sensing or vehicle-based explicit sensing, we then have two different sets of observations upon CL. In this case, two sets of CL data are complementary to each other if one (i.e., vehicle-based explicit sensing) lacks enough coverage rates under a specific temporal period and the other (i.e., cellphone-based implicit sensing) lacks accurate measurements. The truth discovery-based data fusion here functions as the tool to find the truth CL conditions on road segments. In particular, we convert speeds of cellular users and vehicles to CLs according to a standard provided by the navigation service provider, which considers both road segments types and corresponding speed limits. We then have two sets of CL data from implicit signaling data and explicit GPS data. After implementing the method in Section 3 by `scipy.optimize` in Python, we can obtain the optimized CL results built upon two inferred CL datasets.

Similarly, we also evaluate this method at two different levels, i.e., road segments level, and region level. On the road segments level, we still use the four representative road segments as an example to present the performance, the results are shown in the Table 4. The estimation results here are directly calculated CLs by using individual cellphone-based implicit sensing or vehicle-based explicit sensing. For the signaling data, we infer the CLs from traces of moving users and their average travel time; for the GPS data, we obtain the results from users' speeds and convert speeds into CLs based on given standards. We find that, generally, MAPE values decrease by using our proposed data fusion method upon both sensing datasets.

Table 4. Comparison of CL Estimation and Prediction

	MAPE	Road1	Road2	Road3	Road4
Estimate	GPS (%)	56.3	57.6	42.3	11.1
	Signaling (%)	31.9	14.6	20.8	23.6
	Fusion (%)	21.0	13.2	17.7	8.5
Predict	GPS (%)	29.5	32.1	37.5	7.1
	Signaling (%)	30.3	32.1	37.9	11.5
	Fusion (%)	27.9	32.0	36.9	6.5

We also fuse the two data sources on the Voronoi region level. In particular, based on a specific data source (e.g., the cellphone signaling data), we aggregate estimated CLs from different road segments on the same Voronoi region based on the method introduced in Section 2.4. For each region, we calculate a comprehensive CL by considering all road segments within this region and put weights on them based on the road segment length in this region. We then perform a similar process based on the other data source (e.g., the vehicular GPS data), and, finally, we obtain the fused CLs based on the data fusion method and two inferred CLs data as the final results. The results are shown in Figure 35. We find that by considering both two datasets as an integrated sensing approach, it outperforms both individual sensing approaches based on GPS or signaling data alone.

## 5 DISCUSSIONS AND LESSONS LEARNED

In this section, we discuss a few insights we obtained in our measurement study and some lessons learned.

**Limitations:** In this work, we only use data from a particular city (Hefei) for the measurement investigation of explicit and implicit traffic sensing, so the results and conclusions obtained in this work may only apply to Hefei and cities with similar features, e.g., spatiotemporal coverage of data, updating frequency of data, population distribution, and so on. We believe if the key factors such as data distribution of vehicular and cellular sources, and contextual information are similar among cities, our results then can be generalized to other cities, because they are the basis of all the above analyses. Additionally, there are works showing the feasibility of cross-city transfer learning schemes [46]. It has been shown that knowledge can be transferred from the city with sufficient multimodal data and labels to cities with scarce data and labels. In our setting, a similar solution can be proposed, since cities have common data types such as road networks, vehicular networks, and cellular networks. Knowledge learned in the source city, such as relationships among traffic status and contextual data, may be beneficial for traffic investigation of the target city, considering the availability of common contextual data. We will not discuss it in detail in this article but these works show a potential solution to our generalization issue. Further, we study the traffic conditions based on pre-defined spatial partitions, which may not be the optimal partition for traffic condition modeling. However, in general, how to partition cities into different regions to understand traffic conditions or human mobility is still an open question [3]. Last, we only focus on one traffic sensing scenario to explore the pros and cons of explicit and implicit sensing, while our framework can also be applied in other sensing scenarios enabled by multiple sensing systems.

**Spatial Coverage:** As shown in Figures 8, cellular and vehicular networks have different spatial coverage. In general, cellular networks as an example of implicit sensing have better spatial coverage than vehicular networks as an example of explicit sensing. However, the spatial coverage of cellular networks is fixed because of the stationary nature of cell towers. In contrast, the spatial coverage of vehicular networks is dynamic due to the mobile nature of vehicles. This indicates cellular networks can cover more regions, but vehicular networks are more flexible.

**Temporal Coverage:** As shown in Figures 8, we find that for cellular networks as implicit sensing, their temporal coverage is very high for some regions, indicating cellular networks always have data for these regions. However, for some remote regions, if there is no cell tower deployed in these regions, their temporal coverage is always 0. In contrast, for vehicular networks as explicit sensing, they have covered almost all regions, but the distribution is non-uniform, e.g., lots of regions with 20 slots covered among 288 slots, making it less ideal for continuous modeling. The temporal coverage share some similarities to spatial coverage, where explicit sensing is flexible with lower spatiotemporal coverage and implicit sensing is more fixed with higher spatiotemporal coverage.

**Performance Comparison:** We find that the prediction results for crowdedness levels by explicit sensing and implicit sensing approaches have their advantages and disadvantages, in terms of coverage and accuracy. Which approach to use should be based on a set of factors related to system availability, cost, granularity, and so on. Our study reveals some advantages of either explicit or implicit sensing in some concrete settings, including different locations, time slots, time of day, different contextual factors. The details can be found among measurement results.

**Data Collection:** All the data used in this project are legally collected by the service providers. The data from commercial vehicles are collected by a logistics company that owns and manages these vehicles. The private vehicle data are collected by a large insurance company by an onboard device and smartphone app, and all customers are informed about data collection and agreed to provide their data for the company and its business partners for business analyses. In return, they received monthly premium reductions. Finally, all the cellular signaling data are also collected under the consent of cellphone users by signing the contracts.

**More Implicit and Explicit Sensing:** Due to limited data access, we only consider a cellular network as an example of implicit sensing and a vehicular network as an example of explicit sensing. However, our framework can also be generalized by other real-world datasets, which can be treated as explicit and implicit sensing data. We aim to further explore other urban systems to improve our analysis if the system users opt to participate under privacy-preserving mechanisms, e.g., (i) image data from the traffic cameras or the cameras inside the transit systems as implicit sensing. (ii) data of a growing bicycle network with 8,000 bicycles in Hefei for rentals using the smart transaction cards as implicit sensing. (iii) CDR data and cellular traffic data collected from telecommunication systems. The idea can also be generalized to other sensing applications, such as noise pollution sensing and air quality sensing. Take noise pollution as an example, sound sensors can be treated as explicit sensing, since they can directly provide the measurements of noise. While contents from social networks could be a source of implicit sensing, such as people are posting content about gathering somewhere for an outdoor concert, which potentially increases the noise level nearby.

**Privacy:** While understanding traffic condition is beneficial for city residents, we have to protect the privacy of involved residents, i.e., cellphone users and vehicle drivers. All the data used in this project are legally collected by the service providers. For example, signaling data are collected by the cellular provider with the consent of users when they subscribe to the services, which aim to provide better user experience based on the collected data. GPS data from vehicles are collected by the insurance company, which provides a premium discount for users. We only have access to the data from those whom signed the data privacy policy. The partial policy of cellular data usage is attached here for demonstration: “To make sure that you can enjoy our services and to accurately calculate service fees, we will use the collected information under the following cases: To improve your service experience and service quality, or deal with your consulting, complaints, reports, and so on, or to recommend better or more suitable services, we will use your information for the purpose of our products or services under the constraint of this privacy policy.” In this project, all

data analyzed are anonymized by the data provider and we as researchers do not have access to the raw data. During our project, we respect the privacy of users, and the raw data have not been moved from the cellular providers' internal server. There is little risk for the users when the data are used for aggregated traffic sensing. All user IDs have been hashed into global identifiers by the cellular providers' staff, and we cannot leverage these identifiers to trace back to any cellular users; we only access and process data related to traffic condition modeling, non-relevant information is deleted by the provider to reduce risk; finally, in this work, all our results on traffic conditions are given at aggregated cell tower or road segment levels instead of location for a specific timestamp, thus individuals information is not revealed and studied.

## 6 RELATED WORK

In general, there are many approaches to estimate and predict real-time traffic conditions based on different sensing systems and their data. In this article, we divide them into two categories, i.e., explicit sensing and implicit sensing.

**Explicit Sensing:** To explicitly sense the traffic conditions, many systems have been proposed. There are online map services, e.g., Google Map [17] and Gaode Map [16], which are mostly based on crowd-sourcing and smartphone apps. They utilize their users' GPS locations and speeds to model and predict traffic speeds with good accuracy. Another major direction is about onboard GPS devices in both private cars and commercial vehicles such as taxis [3], buses [57], and trucks [6, 36]. In particular, Aslam et al. [1] present a system to use taxis as roving sensors to infer city-scale traffic conditions. They conduct a case study to demonstrate that it is possible to accurately infer traffic volume through data collected from a roving sensor network of taxi probes that log their locations and speeds at regular intervals. Their model and inference procedures can be used to analyze traffic patterns and conditions from historical data, as well as to infer current patterns and conditions from data collected in real time. Besides, traffic infrastructures (such as loop sensors and traffic cameras) are the most direct methods for traffic volume and traffic speed modeling [11]. For example, researchers propose various models for traffic estimation based on the image data obtained by traffic cameras and achieved high accuracy [9, 26]. There are also some works based on social networks relying on human beings as data sources, e.g., researchers utilize traffic information on Twitter [45] for congestion estimation. Xie et al. [48] make use of a vehicle-to-vehicle scheme, i.e., using information shared by other vehicles to estimate the speed of the target vehicles. All these above works make use of sensing sources directly related to traffic sensing, such as traffic speed, travel time, or traffic congestion. However, as we show in our measurement results, these solutions have fundamental problems including low penetration rates and uncertain mobility patterns of sensing devices, e.g., vehicles and smartphone users.

**Implicit Sensing:** The key rationale for implicit sensing is low-cost data collection and high spatiotemporal coverage. For example, the telecommunication infrastructure has been utilized to infer traffic conditions given that there are already massive datasets collected from telecommunication systems, e.g., CDR [44], WiFi data [41], signaling data [10, 22, 23], and so on. These datasets reveal coarse-grained locations and time associated with these locations, which can be used to infer traffic conditions. Moreover, these infrastructure data are almost free, since they are automatically collected by existing infrastructures [13]. Considering the ubiquity of cellphones, cellular data thus have extremely high spatiotemporal rates. There are data records as long as there are people with cellphones and they even do not have to use their cellphones. For example, the first set of work utilizing cellular data [34] to estimate the traffic conditions is based on the idea of utilizing mobile phones as traffic probes, because this infrastructure is already in place in most urban areas, e.g., traffic speed information can be obtained by passively monitoring data transmission in the cellular network. Further, Janecek et al. [22, 23] utilize signaling data from both active and inactive

cellphone users to infer traffic jam and achieved gain in coverage and accuracy by performing two-stage estimation on signaling data. They propose a real-time monitoring and estimation system to improve the response time. Besides, WiFi Access Points are also used as an infrastructure to help to extract the trajectory of users, then based on the connection records of the users, their traveling speed and travel time are estimated [41]. More recently, Derrmann et al. [10] have shown that profile functions of partitions of cellphone networks exist and they exhibit the predictive power of estimating traffic conditions. Moreover, some work even utilizes building occupancy data to infer the traffic conditions of nearby road segments by exploring the correlation between resident density and traffic conditions [13].

**Summary:** As we have shown in our work, both of these two approaches have their distinctive strengths and weaknesses, and we need to carefully examine features of a particular city and sensing infrastructures for the best results of traffic modeling in a real-world setting.

## 7 CONCLUSION

In this article, by designing and implementing EXIMIUS, we utilize two large-scale urban systems and traffic crowdedness level as examples to quantify, measure, and understand both explicit and implicit urban sensing approaches. Our EXIMIUS is based on a three-million-user cellphone network and a five-thousand-vehicle network along with their 1-TB log data and various context data to provide a few novel insights on explicit and implicit urban sensing. Based on our measurements and comparative results in Hefei, we share a few lessons learned, which we believe will help fellow researchers when choosing from explicit and implicit urban sensing approaches. First, neither explicit vehicle-based sensing nor implicit cellphone-based sensing can provide both high spatiotemporal coverage and high accuracy for traffic crowdedness level modeling. The explicit vehicle-based sensing has better accuracy whereas implicit cellphone-based sensing has higher spatiotemporal coverage. Second, various urban context information, e.g., population, road types, the time of day, functions of regions, can provide additional accuracy and coverage, but their impacts on explicit vehicle-based sensing and implicit cellphone-based sensing are quite different. Last, we show that a truth discovery-based data fusion approach by combining explicit vehicle-based sensing and implicit cellphone-based sensing can provide significant improvements for both spatiotemporal coverage and accuracy.

## ACKNOWLEDGMENTS

We thank the editors and reviewers for the detailed and insightful feedback for this work.

## REFERENCES

- [1] Javed Aslam, Sejoon Lim, Xinghao Pan, and Daniela Rus. 2012. City-scale traffic estimation from a roving sensor network. In *Proceedings of the 10th ACM Conference on Embedded Network Sensor Systems*. ACM, 141–154.
- [2] Franz Aurenhammer. 1991. Voronoi diagrams: A survey of a fundamental geometric data structure. *ACM Comput. Surv.* 23, 3 (1991), 345–405.
- [3] Rajesh Krishna Balan, Khoa Xuan Nguyen, and Lingxiao Jiang. 2011. Real-time trip information service for a large taxi fleet. In *Proceedings of the 9th International Conference on Mobile Systems, Applications, and Services*. ACM, 99–112.
- [4] Hugo Barbosa, Marc Barthelemy, Gourab Ghoshal, Charlotte R. James, Maxime Lenormand, Thomas Louail, Ronaldo Menezes, José J. Ramasco, Filippo Simini, and Marcello Tomasini. 2018. Human mobility: Models and applications. *Phys. Rep.* 734 (2018), 1–74.
- [5] Dimitri P. Bertsekas. 1997. Nonlinear programming. *J. Operat. Res. Soc.* 48, 3 (1997), 334–334.
- [6] Pablo Samuel Castro, Daqing Zhang, and Shijian Li. 2012. Urban traffic modelling and prediction using large scale taxi GPS traces. In *Proceedings of the International Conference on Pervasive Computing*. Springer, 57–72.
- [7] C. L. Philip Chen, Jin Zhou, and Wei Zhao. 2012. A real-time vehicle navigation algorithm in sensor network environments. *IEEE Trans. Intell. Transport. Syst.* 13, 4 (2012), 1657–1666.

- [8] Yun Cheng, Kaifei Chen, Ben Zhang, Chieh-Jan Mike Liang, Xiaofan Jiang, and Feng Zhao. 2012. Accurate real-time occupant energy-footprinting in commercial buildings. In *Proceedings of the 4th ACM Workshop on Embedded Sensing Systems for Energy-Efficiency in Buildings*. ACM, 115–122.
- [9] Rita Cucchiara, Massimo Piccardi, and Paola Mello. 2000. Image analysis and rule-based reasoning for a traffic monitoring system. *IEEE Trans. Intell. Transport. Syst.* 1, 2 (2000), 119–130.
- [10] Thierry Derrmann, Raphaël Frank, Francesco Viti, and Thomas Engel. 2017. Estimating urban road traffic states using mobile network signaling data. In *Abstract Book of the 20th International Conference on Intelligent Transportation Systems*.
- [11] Rong Du, Cailian Chen, Bo Yang, Ning Lu, Xinpeng Guan, and Xuemin Shen. 2015. Effective urban traffic monitoring by vehicular sensor networks. *IEEE Trans. Vehic. Technol.* 64, 1 (2015), 273–286.
- [12] Zhihan Fang, Boyang Fu, Zhou Qin, Fan Zhang, and Desheng Zhang. 2020. PrivateBus: Privacy identification and protection in large-scale bus wifi systems. *Proceedings of the ACM on Interactive, Mobile, Wearable and Ubiquitous Technologies* 4, 1 (2020), 1–23.
- [13] Miao Fu, J. Andrew Kelly, and J. Peter Clinch. 2017. Estimating annual average daily traffic and transport emissions for a national road network: A bottom-up methodology for both nationally-aggregated and spatially-disaggregated results. *J. Transport Geogr.* 58 (2017), 186–195.
- [14] Raghu Ganti, Iqbal Mohamed, Ramya Raghavendra, and Anand Ranganathan. 2011. Analysis of data from a taxi cab participatory sensor network. In *Proceedings of the International Conference on Mobile and Ubiquitous Systems: Computing, Networking, and Services*. Springer, 197–208.
- [15] Yan Gao, Kishore Swaminathan, Zhiyong Cui, and Lu Su. 2015. Predictive traffic assignment: A new method and system for optimal balancing of road traffic. In *Proceedings of the 2015 IEEE 18th International Conference on Intelligent Transportation Systems (ITSC'15)*. IEEE, 400–407.
- [16] Gaode. 2017. Gaode Map. Retrieved from <https://ditu.amap.com>.
- [17] Google. 2017. Google Map. Retrieved from <https://www.google.com/maps>.
- [18] Hadi Habibzadeh, Zhou Qin, Tolga Soyata, and Burak Kantarci. 2017. Large-scale distributed dedicated-and non-dedicated smart city sensing systems. *IEEE Sens. J.* 17, 23 (2017), 7649–7658.
- [19] Mordechai Haklay and Patrick Weber. 2008. Openstreetmap: User-generated street maps. *IEEE Perv. Comput.* 7, 4 (2008), 12–18.
- [20] Yutaka Inoue, Akio Sashima, Takeshi Ikeda, and Koichi Kurumatani. 2008. Indoor emergency evacuation service on autonomous navigation system using mobile phone. In *Proceedings of the 2nd International Symposium on Universal Communication (ISUC'08)*. IEEE, 79–85.
- [21] Tiziano Inzerilli, Anna Maria Vagni, Alessandro Neri, and Roberto Cusani. 2008. A location-based vertical handover algorithm for limitation of the ping-pong effect. In *Proceedings of the IEEE International Conference on Wireless and Mobile Computing Networking and Communications (WIMOB'08)*. IEEE, 385–389.
- [22] Andreas Janecek, Karin A. Hummel, Danilo Valerio, Fabio Ricciato, and Helmut Hlavacs. 2012. Cellular data meet vehicular traffic theory: Location area updates and cell transitions for travel time estimation. In *Proceedings of the 2012 ACM Conference on Ubiquitous Computing*. ACM, 361–370.
- [23] Andreas Janecek, Danilo Valerio, Karin Anna Hummel, Fabio Ricciato, and Helmut Hlavacs. 2015. The cellular network as a sensor: From mobile phone data to real-time road traffic monitoring. *IEEE Trans. Intell. Transport. Syst.* 16, 5 (2015), 2551–2572.
- [24] Meng Jin, Yuan He, Dingyi Fang, Xiaojiang Chen, Xin Meng, and Tianzhang Xing. 2018. iGuard: A real-time anti-theft system for smartphones. *IEEE Trans. Mobile Comput.* 17, 10 (2018), 2307–2320.
- [25] Gorkem Kar, Hossen Mustafa, Yan Wang, Yingying Chen, Wenyuan Xu, Marco Gruteser, and Tam Vu. 2014. Detection of on-road vehicles emanating gps interference. In *Proceedings of the ACM SIGSAC Conference on Computer and Communications Security*. ACM, 621–632.
- [26] Li Li, Long Chen, Xiaofei Huang, and Jian Huang. 2008. A traffic congestion estimation approach from video using time-spatial imagery. In *Proceedings of the 1st International Conference on Intelligent Networks and Intelligent Systems (ICINIS'08)*. IEEE, 465–469.
- [27] Yaliang Li, Jing Gao, Chuishi Meng, Qi Li, Lu Su, Bo Zhao, Wei Fan, and Jiawei Han. 2016. A survey on truth discovery. *ACM Sigkdd Explor. Newslett.* 17, 2 (2016), 1–16.
- [28] Siyuan Liu, Yunhuai Liu, Lionel Ni, Minglu Li, and Jianping Fan. 2013. Detecting crowdedness spot in city transportation. *IEEE Trans. Vehic. Technol.* 62, 4 (2013), 1527–1539.
- [29] Chuishi Meng, Yu Cui, Qing He, Lu Su, and Jing Gao. 2017. Travel purpose inference with GPS trajectories, POIs, and geo-tagged social media data. In *Proceedings of the 2017 IEEE International Conference on Big Data (Big Data'17)*. IEEE, 1319–1324.
- [30] Hessam Mohammadmoradi, Omprakash Gnawali, David Moss, Rainer Boelzle, and Gene Wang. 2017. Effectiveness of a task-based residential energy efficiency program in oahu. In *Sustainable Internet and ICT for Sustainability (SustainIT'17)*. IEEE, 1–8.

- [31] S. Papaioannou, A. Markham, and N. Trigoni. 2017. Tracking people in highly dynamic industrial environments. *IEEE Trans. Mobile Comput.* 16, 8 (2017), 2351–2365.
- [32] Zhou Qin, Fang Cao, Yu Yang, Shuai Wang, Yunhuai Liu, Chang Tan, and Desheng Zhang. 2020. CellPred: A behavior-aware scheme for cellular data usage prediction. *Proc. ACM Interact. Mobile Wear. Ubiquitous Technol.* 4, 1 (2020), 1–24.
- [33] Zhou Qin, Yikun Xian, Fan Zhang, and Desheng Zhang. 2020. MIMU: Mobile wifi usage inference by mining diverse user behaviors. *Proc. ACM Interact. Mobile Wear. Ubiquitous Technol.* 4, 4 (2020), 1–22.
- [34] Geoff Rose. 2006. Mobile phones as traffic probes: Practices, prospects and issues. *Transport Rev.* 26, 3 (2006), 275–291.
- [35] Sami Abdulla Mohsen Saleh, Shahrel Azmin Suandi, and Haidi Ibrahim. 2015. Recent survey on crowd density estimation and counting for visual surveillance. *Eng. Appl. Artif. Intell.* 41 (2015), 103–114.
- [36] Qi Shi and Mohamed Abdel-Aty. 2015. Big data applications in real-time traffic operation and safety monitoring and improvement on urban expressways. *Transport. Res. C: Emerg. Technol.* 58 (2015), 380–394.
- [37] Yiwei Song, Yunhuai Liu, Wenqing Qiu, Zhou Qin, Chang Tan, Can Yang, and Desheng Zhang. 2020. MIFF: Human mobility extractions with cellular signaling data under spatio-temporal uncertainty. *Proc. ACM Interact. Mobile Wear. Ubiquitous Technol.* 4, 4 (2020), 1–19.
- [38] statista. 2017. Number of Internet Users Who Used the Internet for Route Planning, to Access Maps or Road Maps (e.g. Google Maps) in Germany from 2013 to 2016, by Frequency (in Millions). Retrieved from <https://www.statista.com/statistics/432169/online-route-planning-and-map-usage-eg-google-maps-germany>.
- [39] Andrew J. Tatem. 2017. WorldPop, open data for spatial demography. *Sci. Data* 4, 1 (2017), 1–4.
- [40] Arvind Thiagarajan, Lenin Ravindranath, Hari Balakrishnan, Samuel Madden, and Lewis Girod. 2011. Accurate, low-energy trajectory mapping for mobile devices.
- [41] Arvind Thiagarajan, Lenin Ravindranath, Katrina LaCurts, Samuel Madden, Hari Balakrishnan, Sivan Toledo, and Jakob Eriksson. 2009. VTrack: Accurate, energy-aware road traffic delay estimation using mobile phones. In *Proceedings of the 7th ACM Conference on Embedded Networked Sensor Systems*. ACM, 85–98.
- [42] US DOT. 2017. CV Pilots Take Advantage of Multiple Communication Media. Retrieved from [https://www.its.dot.gov/pilots/cvp\\_media.htm](https://www.its.dot.gov/pilots/cvp_media.htm).
- [43] De Wang, Weijing Zhong, Zhenxuan Yin, Dongcan Xie, and Xiao Luo. 2018. Spatio-temporal dynamics of population in shanghai: A case study based on cell phone signaling data. In *Big Data Support of Urban Planning and Management*. Springer International Publishing, 239–254.
- [44] Huayong Wang, Francesco Calabrese, Giusy Di Lorenzo, and Carlo Ratti. 2010. Transportation mode inference from anonymized and aggregated mobile phone call detail records. In *Proceedings of the 2010 13th International IEEE Conference on Intelligent Transportation Systems (ITSC'10)*. IEEE, 318–323.
- [45] Senzhang Wang, Lifang He, Leon Stenneth, Philip S. Yu, and Zhoujun Li. 2015. Citywide traffic congestion estimation with social media. In *Proceedings of the 23rd SIGSPATIAL International Conference on Advances in Geographic Information Systems*. ACM, 34.
- [46] Ying Wei, Yu Zheng, and Qiang Yang. 2016. Transfer knowledge between cities. In *Proceedings of the 22nd ACM SIGKDD International Conference on Knowledge Discovery and Data Mining*, 1905–1914.
- [47] Jie Wu, Kun Li, Yifei Jiang, Qin Lv, Li Shang, and Yihe Sun. 2011. Large-scale battery system development and user-specific driving behavior analysis for emerging electric-drive vehicles. *Energies* 4, 5 (2011), 758–779.
- [48] Xiaoyang Xie, Yu Yang, Zhihan Fang, Guang Wang, Fan Zhang, Fan Zhang, Yunhuai Liu, and Desheng Zhang. 2018. coSense: Collaborative urban-scale vehicle sensing based on heterogeneous fleets. *Proc. ACM Interact. Mobile Wear. Ubiquitous Technol.* 2, 4 (2018), 196.
- [49] Xiaoyang Xie, Fan Zhang, and Desheng Zhang. 2018. PrivateHunt: Multi-source data-driven dispatching in for-hire vehicle systems. *Proc. ACM Interact. Mobile Wear. Ubiquitous Technol.* 2, 1 (2018), 45.
- [50] Jungkeun Yoon, Brian Noble, and Mingyan Liu. 2007. Surface street traffic estimation. In *Proceedings of the 5th International Conference on Mobile Systems, Applications and Services*. ACM, 220–232.
- [51] Hui Zang and Jean Bolot. 2011. Anonymization of location data does not work: A large-scale measurement study. In *Proceedings of the 17th Annual International Conference on Mobile Computing and Networking*. ACM, 145–156.
- [52] Desheng Zhang, Juanjuan Zhao, Fan Zhang, and Tian He. 2015. UrbanCPS: A cyber-physical system based on multi-source big infrastructure data for heterogeneous model integration. In *Proceedings of the ACM/IEEE 6th International Conference on Cyber-Physical Systems*. ACM, 238–247.
- [53] Tan Zhang, Ning Leng, and Suman Banerjee. 2014. A vehicle-based measurement framework for enhancing white-space spectrum databases. In *Proceedings of the 20th Annual International Conference on Mobile Computing and Networking*. ACM, 17–28.
- [54] Yiran Zhao, Shen Li, Shaohan Hu, Lu Su, Shuochao Yao, Huajie Shao, Hongwei Wang, and Tarek Abdelzaher. 2017. Greendrive: A smartphone-based intelligent speed adaptation system with real-time traffic signal prediction. In *Proceedings of the 2017 ACM/IEEE 8th International Conference on Cyber-Physical Systems (ICCPs'17)*. IEEE, 229–238.

- [55] Zimu Zheng, Dan Wang, Jian Pei, Yi Yuan, Cheng Fan, and Fu Xiao. 2016. Urban traffic prediction through the second use of inexpensive big data from buildings. In *Proceedings of the 25th ACM International Conference on Information and Knowledge Management*. ACM, 1363–1372.
- [56] Pengfei Zhou, Yuanqing Zheng, and Mo Li. 2012. How long to wait?: predicting bus arrival time with mobile phone based participatory sensing. In *Proceedings of the 10th International Conference on Mobile Systems, Applications, and Services*. ACM, 379–392.
- [57] Pengfei Zhou, Yuanqing Zheng, and Mo Li. 2014. How long to wait? Predicting bus arrival time with mobile phone based participatory sensing. *IEEE Trans. Mobile Comput.* 13, 6 (2014), 1228–1241.
- [58] Yanmin Zhu, Chao Chen, and Min Gao. 2013. An evaluation of vehicular networks with real vehicular GPS traces. *EURASIP J. Wireless Commun. Network*. 2013, 1 (2013), 190.

Received January 2020; revised July 2020; accepted April 2021